On the connection between the self-sputter yield and deposition rate in HiPIMS operation

J. T. Guðmundsson[1,2], M. Rudolph[3], K. Barynova[1], J. Fischer[4], S. Suresh Babu[1], N. Brenning[2,4], M. A. Raadu[2], and D. Lundin[4]

[1] Science Institute, University of Iceland, Reykjavik, Iceland
[2] KTH Royal Institute of Technology, Stockholm, Sweden
[3] Leibniz Institute of Surface Engineering (IOM), Leipzig, Germany
[4] Plasma and Coatings Physics, Linköping University, Sweden

77th Gaseous Electronics Conference,
San Diego, California

October 3, 2024

Introduction – Magnetron sputtering

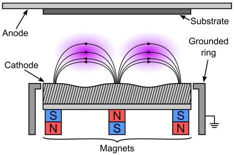

Gudmundsson and Lundin (2020) in High Power Impulse Magnetron Sputtering Discharge, Elsevier, 2020

- Magnetron sputtering has been a highly sucessfull technique that is essential in a number of industrial applications Gudmundsson (2020) PSST **29** 113001
- In a high power impulse magnetron sputtering (HiPIMS) the discharge is driven by high power pulses of low repetition frequency, and with low duty cycle
- This results in high discharge current density, increased electron density, and increased ionization of the sputtered species Gudmundsson et al. (2012) JVSTA **30** 030801

Introduction – Magnetron sputtering

- The film mass density is always higher when deposited with HiPIMS
- The films typically exhibit better crystallinity, and overall improved film properties
- There is a drawback: The deposition rate is lower for HiPIMS when compared to dcMS operated at the same average power
- Many of the ions of the target material are attracted back to the target surface by the cathode potential

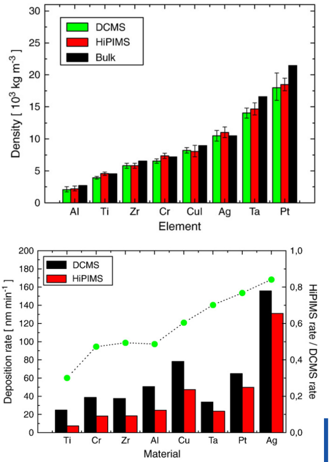

From Samuelsson et al. (2010) SCT **202** 591

Overview

- The ionization region model (IRM)
- Deposition rate vs ionized flux fraction
- Working gas rarefaction
- Summary

The ionization region model (IRM)

Ionization region model

- The ionization region model (IRM) is a time-dependent volume averaged plasma chemical model of the ionization region (IR) of the HiPIMS discharge
- The IRM gives the temporal evolution of the densities of ions, neutrals and electrons
- The IRM gives also two internal parameters that are of importance
  - α_{t} – ionization probability
  - β_{t} – back-attraction probability

Detailed model description is given in Huo et al. (2017) JPD **50** 354003

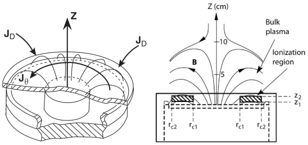

The definition of the volume covered by the IRM

- The IR is defined as an annular cylinder of width $w_{\mathrm{rt}} = r_{\mathrm{c2}} - r_{\mathrm{c1}}$ and thickness $L = z_2 - z_1$, extends from z_1 to z_2 axially away from the target

From Raadu et al. (2011) PSST **20** 065007

Ionization region model

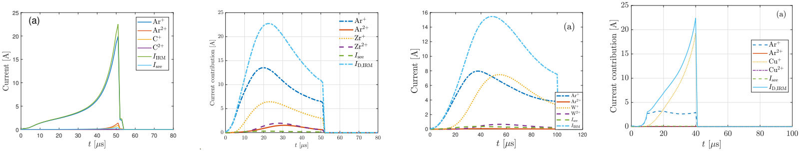

C: PSST (2021) **30** 115017 Zr: JVSTA (2024) **42** 043007 W: PSST (2022) **31** 065009 Cu: SCT (2022) **442** 128189

- The temporal evolution of the discharge current composition at the target surface for three different targets
- With Cu target Cu^+ ions dominate, with graphite target Ar^+ ions dominate
- For Zr and W targets there is a mix of Ar^+ and metal ions

Ionization region model

- For tungsten target the ionization probability α_t increases with increased discharge voltage
- The peak discharge current increases with increased discharge voltage
- Earlier we have argued that the ionization probability depends only on the peak discharge current and increases with increased peak discharge current

Rudolph et al. (2022) JPD **55** 015202

- The back-attraction probability $\beta_{t,pulse}$ decreases with increased discharge voltage

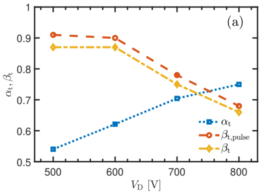

A discharge with a tungsten target

From Suresh Babu et al. (2022) PSST **31** 065009

Ionization region model

- For zirconium target the ionization probability α_{t} increases with increased current density
- The back-attraction probability $\beta_{\mathrm{t,pulse}}$ does not show any trend

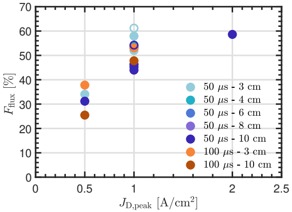

- The measured ionized flux fraction is used to lock the model

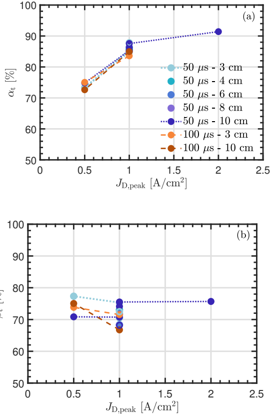

discharge with a zirconium target

From Suresh Babu et al. (2024) JVSTA **42** 043007

Deposition rate vs ionized flux fraction

Deposition rate – α_t and β_t

- We can relate the measured quantities normalized deposition rate $F_{\mathrm{DR,sput}}$ and the ionized flux fraction $F_{\mathrm{ti,flux}}$

$$F_{\mathrm{DR,sput}} = \frac{\Gamma_{\mathrm{DR}}}{\Gamma_0} = (1 - \alpha_t \beta_t)$$

$$F_{\mathrm{ti,flux}} = \frac{\Gamma_{\mathrm{DR,ions}}}{\Gamma_{\mathrm{DR,sput}}} = \frac{\Gamma_0 \alpha_t (1 - \beta_t)}{\Gamma_0 (1 - \alpha_t \beta_t)} = \frac{\alpha_t (1 - \beta_t)}{(1 - \alpha_t \beta_t)}$$

to the internal parameters back attraction probability β_t

$$\beta_t = \frac{1 - F_{\mathrm{DR,sput}}}{1 - F_{\mathrm{DR,sput}}(1 - F_{\mathrm{ti,flux}})}$$

and ionization probability α_t

$$\alpha_t = 1 - F_{\mathrm{DR,sput}}(1 - F_{\mathrm{ti,flux}})$$

Hajihoseini et al. (2019) *Plasma* **2** 201 and later refined by Rudolph et al. (2021) JAP **129** 033303

Deposition rate – Optimization

- There are two measures of how good a HiPIMS discharge is:
  - the fraction $F_{\mathrm{DR,sput}}$ of all the sputtered material that reaches the diffusion region (DR)
  - the fraction $F_{\mathrm{ti,flux}}$ of ionized species in that flux
- There is a trade off between the goals of higher $F_{\mathrm{DR,sput}}$ and higher $F_{\mathrm{ti,flux}}$
- The question that remains:
  - How can we vary the ionization probability α_{t} and maybe more importantly the back-attraction probability β_{t} ?

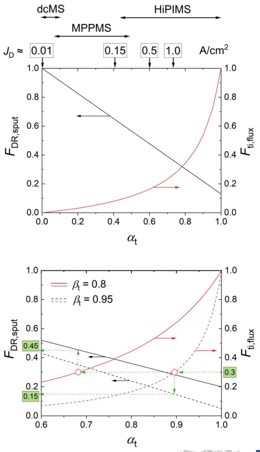

From Brenning et al. (2020) *JVSTA* **38** 033008

Deposition rate – Optimization

- What determines the back-attraction probability ?
- How can one influence the back-attraction probability ?
- The back-attraction probability $\beta_{\rm t,pulse}$, determined by IRM, versus the self-sputter yield for various target materials
- The data indicate that the back-attraction probability decreases roughly linearly with increased self-sputter yield

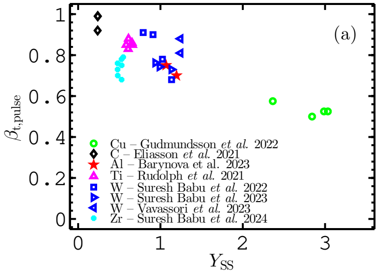

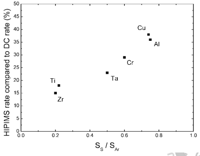

Helmersson et al. (2005) SVC Conf. Proc. 2005, p. 458

Working gas rarefaction

Working gas rarefaction

- The sputtered species enter the discharge at considerable energy, which is determined by the cohesive energy of the solid target
- The interaction between the energetic sputtered particles and the working gas atoms can lead to a reduction in the working gas density – as has been observed experimentally in the HiPIMS discharge
- Working gas rarefaction has been observed in the HiPIMS discharge

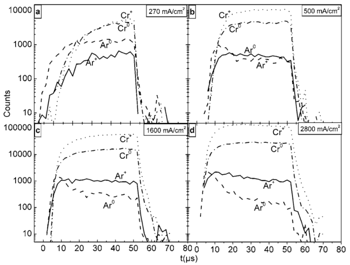

From Alami et al. (2006) APL **89**(15) 154104

Working gas rarefaction

- HiPIMS discharge with graphite target and $J_{\mathrm{D,peak}} = 1$ A cm^{-2}

  Eliasson et al. (2021) PSST **30** 115017

- Argon atoms are lost mainly through electron impact ionization by primary and secondary electrons
- Contributions of kick-out and charge-exchange are negligible
- Diffusion contributes to a net loss of argon atoms during the pulse, but to a flow into the ionization region after the pulse is off

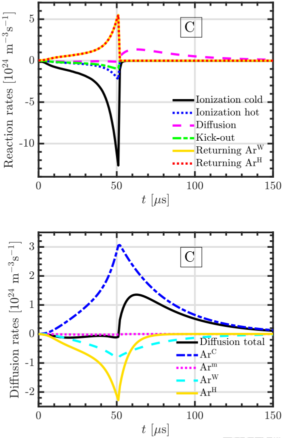

From Barynova et al. PSST **33**(6) 065010

Working gas rarefaction

- HiPIMS discharge with tungsten target and $J_{\mathrm{D,peak}} = 0.54$ A cm^{-3}

  Suresh Babu et al. (2022) PSST **31** 065009

- The main contributor to the loss of argon atoms from the IR is kick-out by tungsten atoms sputtered from the target (39 – 48 % contribution)
- The second most important loss process is electron impact ionization by secondary electrons followed by electron impact ionization by the primary electrons

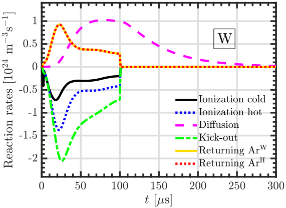

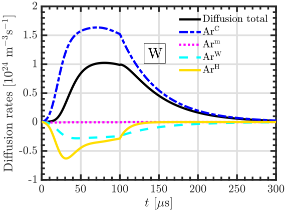

From Barynova et al. PSST **33**(6) 065010

Working gas rarefaction

- The relative contributions of the various processes to working gas rarefaction varies greatly depending on the target material
- The various contributions versus the atomic mass of the target material for $J_{\mathrm{D,peak}} \sim 1$ A/cm^2 and $p_{\mathrm{g}} \sim 1$ Pa

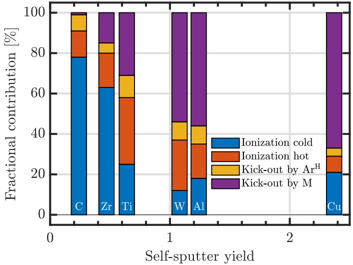

From Barynova et al. PSST **33**(6) 065010

Summary

Summary

- The discharge current composition at the target surface depends on the target material
- There is an inescapable conflict between the goals of higher deposition rate and higher fraction of ionized species in the sputtered material flux
- The back-attraction probability appears to depend on the self-sputter yield – it is lower for higher self-sputter yield
- The main contributor to working gas rarefaction for low sputter yield target is electron impact ionization, while for targets with high sputter yield kick-out by the sputtered species is the main contributor

Thank you for your attention

tumi@hi.is

The slides can be downloaded at

http://langmuir.raunvis.hi.is/~tumi/ranns.html

Further reading

- J. T. Gudmundsson, Physics and technology of magnetron sputtering discharges, Plasma Sources Science and Technology, **29**(11) (2020) 113001

Topical Review

Physics and technology of magnetron sputtering discharges

- J. T. Gudmundsson, André Anders, and Achim von Keudell, Foundations of physical vapor deposition with plasma assistance, Plasma Sources Science and Technology, **31**(8) (2022) 083001

Topical Review

Foundations of physical vapor deposition with plasma assistance

- Daniel Lundin, Tiberiu Minea and Jon Tomas Gudmundsson (eds.), High Power Impulse Magnetron Sputtering: Fundamentals, Technologies, Challenges and Applications, Elsevier, 2020

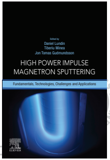

References

Alami, J., K. Sarakinos, G. Mark, and M. Wuttig (2006). On the deposition rate in a high power pulsed magnetron sputtering discharge. *Applied Physics Letters 89*(15), 154104.

Barynova, K., S. Suresh Babu, M. Rudolph, J. Fischer, D. Lundin, M. A. Raadu, N. Brenning, and J. T. Gudmundsson (2024). On working gas rarefaction in high power impulse magnetron sputtering. *Plasma Sources Science and Technology 33*(6), 065010.

Brenning, N., A. Butler, H. Hajihoseini, M. Rudolph, M. A. Raadu, J. T. Gudmundsson, T. Minea, and D. Lundin (2020). Optimization of HiPIMS discharges: The selection of pulse power, pulse length, gas pressure, and magnetic field strength. *Journal of Vacuum Science and Technology A 38*(3), 033008.

Brenning, N., J. T. Gudmundsson, M. A. Raadu, T. J. Petty, T. Minea, and D. Lundin (2017). A unified treatment of self-sputtering, process gas recycling, and runaway for high power impulse sputtering magnetrons. *Plasma Sources Science and Technology 26*(12), 125003.

Eliasson, H., M. Rudolph, N. Brenning, H. Hajihoseini, M. Zanáška, M. J. Adriaans, M. A. Raadu, T. M. Minea, J. T. Gudmundsson, and D. Lundin (2021). Modeling of high power impulse magnetron sputtering discharges with graphite target. *Plasma Sources Science and Technology 30*(11), 115017.

Gudmundsson, J. T. (2020). Physics and technology of magnetron sputtering discharges. *Plasma Sources Science and Technology 29*(11), 113001.

Gudmundsson, J. T., N. Brenning, D. Lundin, and U. Helmersson (2012). The high power impulse magnetron sputtering discharge. *Journal of Vacuum Science and Technology A 30*(3), 030801.

Gudmundsson, J. T. and D. Lundin (2020). Introduction to magnetron sputtering. In D. Lundin, T. Minea, and J. T. Gudmundsson (Eds.), *High Power Impulse Magnetron Sputtering: Fundamentals, Technologies, Challenges and Applications*, pp. 1–48. Amsterdam, The Netherlands: Elsevier.

Hajihoseini, H., M. Čada, Z. Hubička, S. Ünaldi, M. A. Raadu, N. Brenning, J. T. Gudmundsson, and D. Lundin (2019). The effect of magnetic field strength and geometry on the deposition rate and ionized flux fraction in the HiPIMS discharge. *Plasma 2*(2), 201–221.

Held, J., V. Schulz-von der Gathen, and A. von Keudell (2023). Ionization of sputtered material in high power impulse magnetron sputtering plasmas – comparison of titanium, chromium and aluminum. *Plasma Sources Science and Technology 32*(6), 065006.

References

Helmersson, U., M. Lattemann, J. Alami, J. Bohlmark, A. P. Ehiasarian, and J. T. Gudmundsson (2005). High power impulse magnetron sputtering discharges and thin film growth: A brief review. In *Proceedings of the 48th Society of Vacuum Coaters Annual Technical Conferenece*, pp. 458 – 464.

Huo, C., D. Lundin, J. T. Gudmundsson, M. A. Raadu, J. W. Bradley, and N. Brenning (2017). Particle-balance models for pulsed sputtering magnetrons. *Journal of Physics D: Applied Physics 50*(35), 354003.

Magnus, F., A. S. Ingason, S. Olafsson, and J. T. Gudmundsson (2012). Nucleation and resistivity of ultrathin TiN films grown by high power impulse magnetron sputtering. *IEEE Electron Device Letters 33*(7), 1045 – 1047.

Raadu, M. A., I. Axnäs, J. T. Gudmundsson, C. Huo, and N. Brenning (2011). An ionization region model for high power impulse magnetron sputtering discharges. *Plasma Sources Science and Technology 20*(6), 065007.

Rudolph, M., N. Brenning, H. Hajihoseini, M. A. Raadu, T. M. Minea, A. Anders, D. Lundin, and J. T. Gudmundsson (2022). Influence of the magnetic field on the discharge physics of a high power impulse magnetron sputtering discharge. *Journal of Physics D: Applied Physics 55*(1), 015202.

Rudolph, M., H. Hajihoseini, M. A. Raadu, J. T. Gudmundsson, N. Brenning, T. M. Minea, A. Anders, and D. Lundin (2021). On how to measure the probabilities of target atom ionization and target ion back-attraction in high-power impulse magnetron sputtering. *Journal of Applied Physics 129*(3), 033303.

Samuelsson, M., D. Lundin, J. Jensen, M. A. Raadu, J. T. Gudmundsson, and U. Helmersson (2010). On the film density using high power impulse magnetron sputtering. *Surface and Coatings Technology 202*(2), 591–596.

Suresh Babu, S., M. Rudolph, D. Lundin, T. Shimizu, J. Fischer, M. A. Raadu, N. Brenning, and J. T. Gudmundsson (2022). Ionization region model of a high power impulse magnetron sputtering of tungsten. *Plasma Sources Science and Technology 31*(6), 065009.

Suresh Babu, S., J. Fischer, M. Rudolph, D. Lundin, and J. T. Gudmundsson (2024). Modeling of high power impulse magnetron sputtering discharges with a zirconium target. *Journal of Vacuum Science and Technology A 42*(4), 043007.